Am J Cancer Res 2026;16(11):4777-4793
www.ajcr.us /ISSN:2156-6976/ajcr0176067

Original Article

FTO-mediated demethylation of m6A on LINC02473 promotes glycolysis in lung adenocarcinoma cells by suppressing miR-340-5p

Yichi Wang[1*], Chenhong Fu[1*], Yamei Zheng[2], Zhao Li[2], Jiwei Li[2], Yihui Fu[2]

[1]Department of Pulmonary and Critical Care Medicine, Hainan Affiliated Hospital of Hainan Medical University, Haikou, Hainan, P. R. China; [2]Department of Pulmonary and Critical Care Medicine, Hainan General Hospital (Hainan Affiliated Hospital of Hainan Medical University), Haikou, Hainan, P. R. China. [*]Equal contributors.

Received August 17, 2026; Accepted October 14, 2026; Epub November 15, 2026; Published November 30, 2026

Abstract: Lung adenocarcinoma (LUAD) is a major subtype of lung cancer, and its progression involves dysregulated epitranscriptomic modifications. This study aimed to explore the role of fat mass and obesity-associated protein (FTO)-mediated m6A demethylation of the long non-coding RNA LINC02473 and its downstream effects in LUAD. Using GEO datasets (GSE138172 and GSE196584), LINC02473 was found to be elevated in LUAD cells. Gene Set Enrichment Analysis (GSEA) linked high LINC02473 expression to key metabolic pathways, including pyruvate metabolism and glycolysis. Mechanistically, FTO removed the m6A modification from LINC02473, thereby enhancing its stability and expression. Upregulated LINC02473 subsequently suppressed miR-340-5p. Functional assays showed that manipulating LINC02473 expression (knockdown or overexpression) markedly affected LUAD cell proliferation, apoptosis and glycolytic activity. Dual-luciferase reporter assays confirmed that LINC02473 directly targets miR-340-5p. Collectively, FTO stabilizes LINC02473 via m6A demethylation, which in turn inhibits miR-340-5p and promotes glycolysis and malignant progression in LUAD. The FTO/LINC02473/miR-340-5p axis may serve as a potential diagnostic and therapeutic target for LUAD.

Keywords: Lung adenocarcinoma, LINC02473, FTO, m6A, miR-340-5p, glycolysis

Introduction

Lung cancer (LC) remains a leading cause of cancer-related mortality worldwide [1], with lung adenocarcinoma (LUAD) accounting for approximately 40% of all cases [2]. Despite advances in diagnosis and treatment, the prognosis of LUAD remains poor [3], underscoring the need to identify novel molecular mechanisms driving its progression. A deeper understanding of these mechanisms may facilitate the development of targeted therapies and improve clinical outcomes.

With the development of high-throughput sequencing technology along with its analysis techniques, it has been found that protein-coding genes account for less than 2% of the human genome, whereas the vast majority of transcripts are non-coding RNAs (ncRNAs) [4]. Long non-coding RNAs (lncRNAs) are generally more than 200 nucleotides long. These ncRNAs have been increasingly recognized for their active roles in important biological processes such as cell proliferation and migration [5]. Evidence suggests that lncRNAs are involved in regulating biological functions of LC and could be used as biomarkers for diagnosis or therapy in the future [6, 7]. One example of such lncRNA is lncRNA BC069792, whose antiproliferative role in breast cancer development is achieved by the inhibition of KCNQ4 [8]. In addition, lncRNA PKMYT1AR is involved in the activation of the Wnt pathway and, hence, maintains the stemness of non-small cell lung cancer (NSCLC) cells [9]. Another recently discovered lncRNA, LINC02473, requires further exploration to acquire a comprehensive understanding of its function, although preliminary studies suggest its association with the development of LUAD. Elucidating the regulatory mechanism of LINC02473 and its upstream and downstream

https://doi.org/10.62347/BCXQ1818

signaling pathways may provide novel insights into LUAD progression and offer potential targets for diagnosis and treatment.

Gene expression regulation is highly dependent on the process of N6-methyladenosine (m6A), one of the most widespread modifications of mRNA. Its main functions include the regulation of mRNA processing, localization, translation, and degradation [10]. The process of controlling m6A modifications is mainly carried out by methyltransferases and demethylases [11, 12]. These enzymes are responsible for adding or removing methyl groups from the mRNA molecules [11, 12]. In addition to m6A methyltransferases and demethylases, RNA-binding proteins known as m6A readers selectively recognize and interact with m6A-modified transcripts [13]. Together, these three classes of regulatory proteins coordinate m6A-dependent control of RNA metabolism and gene expression. Fat mass and obesity-associated protein (FTO), an important m6A demethylase, removes methyl groups from m6A-modified RNA and thereby modulates RNA stability and translational efficiency [14]. Dysregulated FTO-mediated demethylation has been associated with the pathogenesis of multiple diseases, including cancer [14]. In NSCLC, FTO has also been reported to facilitate metastatic progression by altering m6A modification of FAP and consequently activating integrin/FAK signaling [15]. Accumulating evidence further suggests that m6A modification is involved in the post-transcriptional regulation of lncRNAs. However, whether m6A methylation contributes to the stability or translational regulation of LINC02473 remains unclear [16]. Further investigation is therefore required to define the role of m6A modification in the regulation of LINC02473 and other lncRNAs.

In this context, this work was carried out to elucidate the regulatory function of m6A modification of the LUAD-related lncRNA LINC02473 and FTO-mediated regulation of miR-340-5p expression, as well as their effects on glycolysis and proliferation in LUAD. We hypothesized that FTO-mediated m6A demethylation stabilizes LINC02473, which in turn suppresses miR-340-5p, thereby promoting glycolysis and malignant progression in LUAD. This study may provide novel insights into the molecular mechanisms of LUAD and help identify potential targets for diagnosis and treatment. These findings hold clinical significance for improving the management of LUAD patients.

Materials and methods

Sample information

The Gene Expression Omnibus (GEO) repository provided two datasets, GSE138172 and GSE196584, for the purpose of lncRNA screening. GSE138172 consisted of 10 samples in total, with 5 tumor samples and 5 control samples. Similarly, GSE196584 also consisted of 10 samples, with 5 tumor samples and 5 control samples.

Bioinformatics analysis

We used the R package "limma" [17] to analyze lncRNA expression in the GSE138172 and GSE196584 datasets. Differentially expressed genes were identified using the criteria of $|\log FC| \geq 1$ and adjusted *P*-value (adj.P.Val) < 0.05. The Benjamini-Hochberg method was applied to correct for multiple comparisons. GSEA was conducted to identify enriched biological pathways and Gene Ontology terms, including biological processes, cellular components, and molecular functions, in samples with high versus low LINC02473 expression, aiming to explore the potential mechanisms of LINC02473 in LUAD.

Cell line sources

The immortalized human bronchial epithelial (HBE) cells and three human LUAD cell lines (A549, A427, and PC-9) were procured from the Chinese Academy of Sciences. The LUAD cell lines were cultured in RPMI 1640 medium (11875093, Gibco, USA) supplemented with 10% fetal bovine serum (FBS; A5670701, Gibco, USA) and 1% penicillin-streptomycin (15140122, Gibco, USA).

Transfection of plasmids and siRNAs

Recombinant plasmids for overexpressing LINC02473, AC111152.2, and FTO (pcDNA-LINC02473, pcDNA-AC111152.2, and pcDNA-FTO) and a negative control plasmid (pcDNA-NC) were obtained from GeneChem (Shanghai, China). siRNAs targeting LINC02473, FTO, and AC125603.1 (si-LINC02473, si-FTO, and si-AC125603.1) and a negative control (si-NC)

were synthesized by GenePharma (Shanghai, China). miR-340-5p mimics and the corresponding negative control (miR-NC) were sourced from the Public Protein/Plasmid Library (PPL) (Nanjing, China). Lipofectamine 3000 (L3000015, Invitrogen, USA) was used for plasmid transfection, and INTERFERin (Polyplus, France) was used for siRNA and miRNA mimic transfection.

qRT-PCR

Cells were lysed in TRIzol reagent (15596018, Invitrogen, USA) at 1 mL per 5 × 10^6 cells, and total RNA was isolated according to the manufacturer's instructions. Approximately 1.5 μg of total RNA was reverse-transcribed using the RevertAid First Strand cDNA Synthesis Kit (K1622, Thermo Scientific, USA). qPCR was performed on a QuantStudio™ 6 Flex system (Applied Biosystems, USA) with FastStart Universal SYBR Green Master (ROX) (04913914-001, Roche, Switzerland). The 20 μL reaction mixture contained 10 μL of 2× SYBR Green Master Mix, 1 μL cDNA, 0.5 μL forward primer (10 μM), 0.5 μL reverse primer (10 μM), and 8 μL nuclease-free water. Thermal cycling conditions were 95°C for 10 min, followed by 40 cycles of 95°C for 15 s and 60°C for 60 s. U6 or GAPDH was used as the endogenous reference. The primers for LINC02473 (Forward primer: 5'-AAGACAGTACCCAGAGCAGC-3'; Reverse primer: 5'-TGAAGGTCATCCAGTTGTCAGA-3'), were used for qPCR. All cellular experiments were performed using cells from different passages to ensure biological replicates.

Western blotting (WB)

Cells were lysed in RIPA lysis buffer (P0013K, Beyotime, China) supplemented with 1 mM PMSF and protease inhibitor cocktail (469313-2001, Roche, Switzerland). Protein concentration was determined, and 50 μg of protein per sample was separated by SDS-PAGE and transferred onto a PVDF membrane. The membrane was blocked with 5% skim milk for 2 h and incubated overnight at 4°C with primary antibodies, including anti-FTO (1:1000, ab126605, Abcam, UK) and anti-GAPDH (1:5000, ab181602, Abcam, UK). After three washes with PBS, the membrane was incubated with HRP-conjugated goat anti-rabbit IgG (1:5000, ab97051, Abcam, UK) for 2 h at room temperature. Protein bands were visualized using ECL reagent (WBKLS0500, Millipore, USA) and quantified with ImageJ software. All WB experiments were performed using cells from different passages to ensure biological replicates.

Cell proliferation assay

Cell proliferation was assessed using the Cell Counting Kit-8 (CCK-8, CK04, Dojindo, Japan), 5-ethynyl-2'-deoxyuridine (EdU) incorporation assay (C0071S, Beyotime, China), and colony formation assay. For CCK-8, cells were seeded in 96-well plates, and CCK-8 reagent was added to each well, followed by incubation for 3 h. Absorbance was measured at 450 nm. For EdU staining, cells were incubated with EdU labeling solution for 4 h, fixed with 4% paraformaldehyde (P1110, Solarbio, China), permeabilized with 0.3% Triton X-100 (T9284, Sigma-Aldrich, USA), and then treated with the Click-iT reaction mixture, followed by DAPI (C1005, Beyotime, China) counterstaining. For colony formation, cells were seeded in 12-well plates and cultured for 8-12 days until visible colonies formed. Colonies were fixed, stained with crystal violet (G1063, Solarbio, China), photographed, and counted using ImageJ software.

Flow cytometry analysis

To evaluate cell death by flow cytometry, cells were cultured until they reached the logarithmic growth phase. Apoptotic cells were stained using the FITC Annexin V/PI apoptosis detection kit (556547, BD Biosciences, USA), which contains FITC-conjugated Annexin V and propidium iodide (PI). Stained cells were analyzed on a FACScan flow cytometer (BD Biosciences, USA), and the proportion of apoptotic cells was quantified.

ECAR measurement

Extracellular acidification rate (ECAR) was measured using a Seahorse XF96 Extracellular Flux Analyzer (Agilent, USA) with a Seahorse XF Glycolysis Stress Test Kit (103020-100, Agilent, USA) according to the manufacturer's instructions. Cells were seeded into XF96 cell culture microplates (102601-100, Agilent, USA) and incubated in XF base medium (103335-100, Agilent, USA). Glucose (10 mM), oligomycin (1 μM), and 2-deoxyglucose (2-DG, 50 mM) were then sequentially injected, and ECAR was recorded in mpH/min.

RNA stability assay

Cells were treated with actinomycin D (5 μg/mL, A4262, Sigma-Aldrich, USA). Total RNA was extracted at 0, 3, 6, 9, and 12 h after treatment, and LINC02473 expression was detected by qRT-PCR. The relative remaining RNA level at each time point was tested and normalized to the 0 h value.

Dual luciferase reporter gene assay

To verify the direct binding between LINC02473 and miR-340-5p, the wild-type LINC02473 sequence (LINC02473-WT) and a mutant sequence with the predicted miR-340-5p-binding site mutated (LINC02473-MUT) were cloned into the pGL3-promoter vector for luciferase reporter assays. To evaluate the role of m6A sites, three additional mutant constructs (MUT1, MUT2, and MUT3) were generated by mutating the m6A consensus motifs (DRACH) within LINC02473 and constructed onto the luciferase reporter gene vector. Cells were co-transfected with the reporter plasmids and miR-340-5p mimics or pcDNA-FTO using Lipofectamine 3000. After 48 h, luciferase activity was measured using the Dual-Luciferase Reporter Assay System (E1910, Promega, USA), and the firefly/Renilla ratio was calculated.

RNA immunoprecipitation (RIP) assays

Methylated RIP (MeRIP) was performed using the Magna MeRIP m6A assay kit (17-10499, Millipore, USA) according to the manufacturer's instructions. Briefly, total RNA was fragmented and incubated with protein A/G magnetic beads (88802, Thermo Fisher, USA) pre-conjugated with anti-m6A antibody (1:100; 68055-1-Ig, Proteintech, China). After washing, the immunoprecipitated RNA was eluted, purified by ethanol precipitation, and analyzed by RT-qPCR.

Ago2-RIP was performed using the Magna RIP RNA-binding protein immunoprecipitation kit (17-700, Millipore, USA) following the manufacturer's instructions. A427 and PC-9 cells were lysed and incubated with magnetic beads conjugated with anti-Ago2 antibody (1:100; ab32381, Abcam, UK) or normal IgG at 4°C overnight. The immunoprecipitated RNA was purified and subjected to RT-qPCR to detect the enrichment of LINC02473 and miR-340-5p.

Statistical analysis

Statistical analyses were performed using SPSS version 26.0. Quantitative data are presented as the mean ± standard deviation (SD). All cellular experiments were performed in at least three independent biological replicates. Comparisons between two groups were conducted using Student's t-test when appropriate, whereas differences among three or more groups were assessed by one-way analysis of variance (ANOVA). $P < 0.05$ was considered indicative of statistical significance.

Results

Differential gene screening

Differentially expressed genes were identified in the GSE138172 and GSE196584 datasets. Analysis using the limma package detected 71 upregulated and 19 downregulated genes in GSE138172 (**Figure 1A**, **1B**). In GSE196584, 113 genes were upregulated and 202 were downregulated (**Figure 1C**, **1D**).

Co-expression gene screening

We mapped the common genes that were differentially expressed in the two datasets by means of Venn diagram. First, three co-expressed differentially expressed genes were found in the GSE138172 and GSE196584 datasets by Venn diagram (**Figure 2A**). One of the low-expressed genes was AC111152.2 (**Figure 2B**). And 2 highly expressed genes were AC125603.1 and LINC02473 (**Figure 2C**).

Gene selection and expression validation

After conducting an extensive literature search, we were unable to find any relevant references for AC111152.2, AC125603.1, and LINC02473 genes. Following this, we performed experiments to investigate the expression levels of these three lncRNAs in multiple LUAD cell lines. Compared with normal HBE cells, AC111152.2 showed no significant change in LUAD cells (**Figure 3A**), and AC125603.1 was highly expressed only in PC-9 cells (**Figure 3B**). Notably, LINC02473 was significantly upregulated in A549, A427, and PC-9 cells compared with HBE cells (**Figure 3C**). Among the three, LINC02473 exhibited the most significant change. To fur-

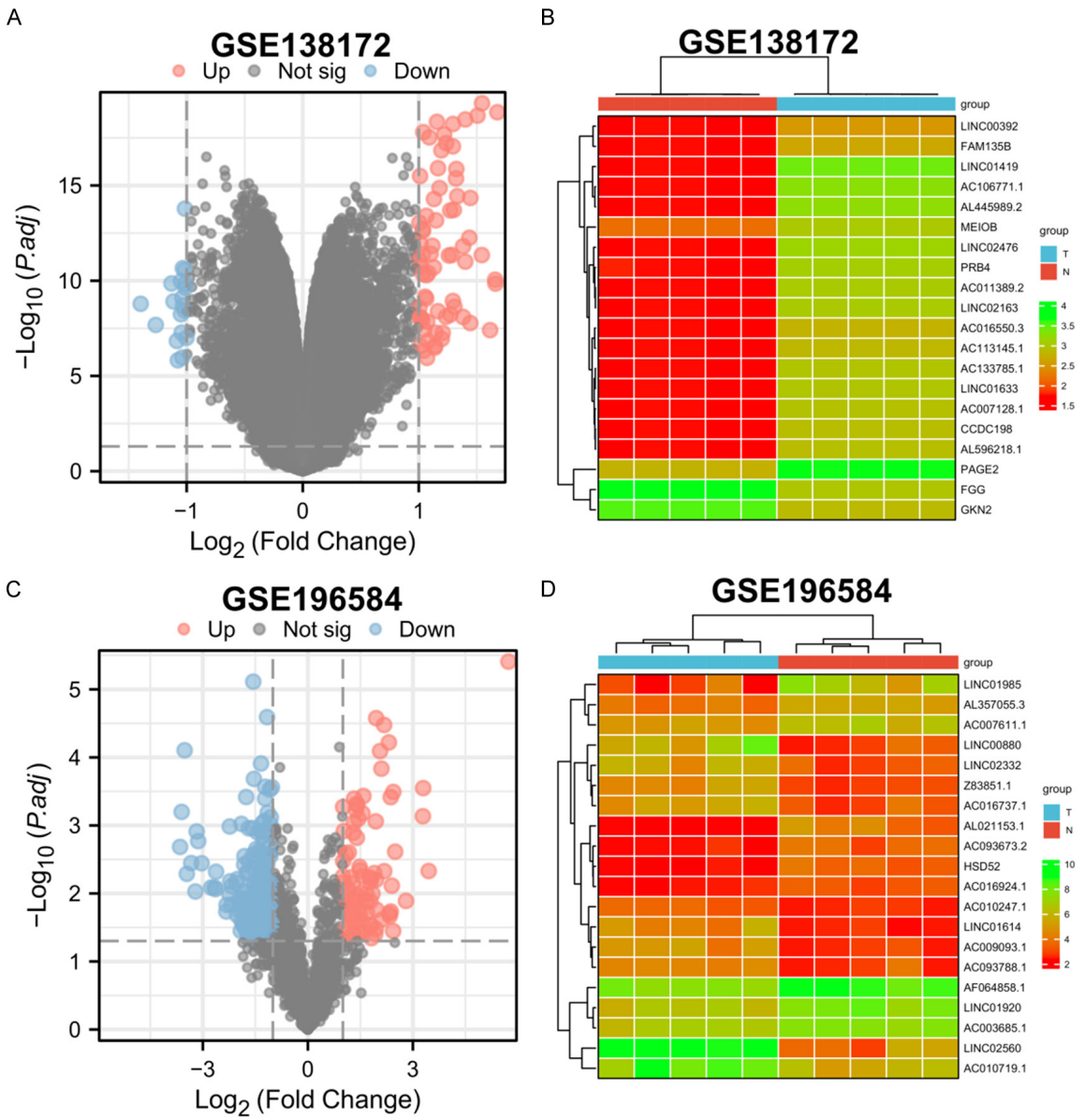


Figure 1. Difference analysis of GSE138172 and GSE196584 datasets. A. Volcano plot demonstrating the distribution of differential genes in the GSE138172 dataset. B. Heatmap demonstrating the expression of the top 20 differential genes in the GSE138172 dataset. C. Volcano plot demonstrating differential gene distribution in GSE196584 dataset. D. Heatmap showing the top 20 differential gene expression in the GSE196584 dataset.

ther rule out potential interference from the other lncRNAs, we examined the effects of AC111152.2 overexpression or AC125603.1 knockdown on LUAD cell viability. The results showed that pcDNA-AC111152.2 significantly upregulated AC111152.2 expression (Figure S1A) but did not affect the viability of A427 or PC-9 cells (Figure S1B). Moreover, si-AC125603.1 significantly reduced AC125603.1 expression (Figure S1C) and similarly did not affect cell viability (Figure S1D). Therefore, we opted to prioritize LINC02473 for further investigation in our study.

GSEA functional enrichment analysis

In order to gain deeper insights into the role of LINC02473, we classified samples into high- and low-LINC02473 expression groups, based on its expression data. Subsequently, we performed GSEA analysis utilizing the GSE196584 dataset. Through KEGG enrichment analysis,

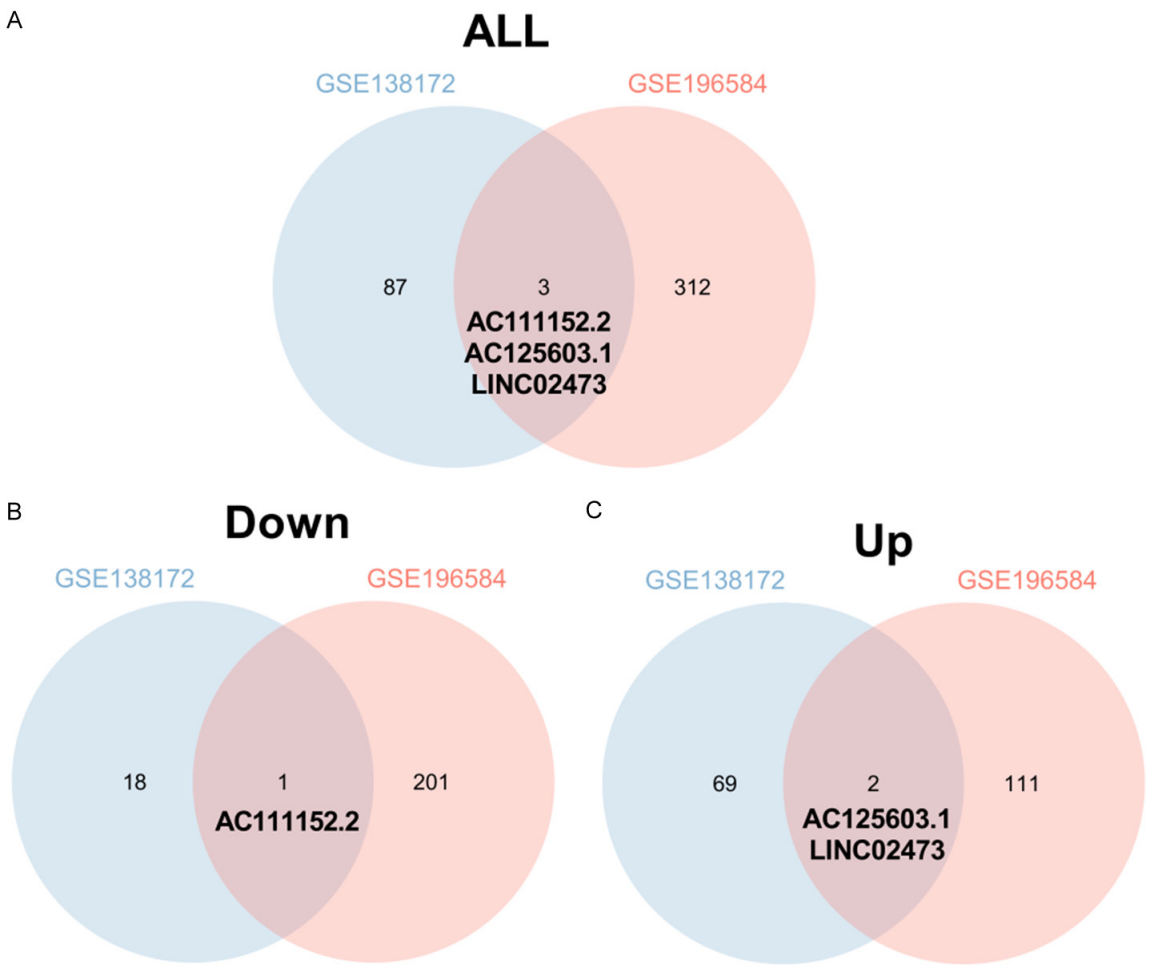


Figure 2. Venn diagram screening for common differential genes. A. Venn diagram screening for common differential genes in both datasets. B. Venn diagram screening for common differential genes with low expression in both datasets. C. Venn diagram screening for common differential genes with high expression in both datasets.

we discovered significant associations between the expression of LINC02473 and pyruvate metabolism, complement and coagulation cascades, as well as glycolysis gluconeogenesis (**Figure 4A**). GO analysis revealed that these enrichment results were mainly related to mitochondria, organelles, cytoskeleton, gene expression, regulation of cellular functions, and related molecular functions (**Figure 4B-D**).

LINC02473 expression validation

To examine the impact of LINC02473 on cellular functions, we initially constructed pcDNA-LINC02473 and si-LINC02473 plasmids for expression validation. Analysis revealed a substantial increase in LINC02473 levels in pcDNA-LINC02473 compared to pcDNA-NC (**Figure 5A**), whereas si-LINC02473 exhibited a significant decrease in LINC02473 levels compared to si-NC (**Figure 5B**). This verified the successful construction of the plasmids. Following this, we introduced the overexpression and repression constructs into A427 and PC-9 cells, and discovered a significant upregulation of LINC02473 in both cell lines upon pcDNA-LINC02473 intervention (**Figure 5C**). Conversely, LINC02473 expression was decreased in si-LINC02473-transfected cells (**Figure 5D**). These findings demonstrate the successful establishment of an in vitro model for further investigation.

Effects on biological functions of LUAD cells after regulation of LINC02473

Interventions were applied to LUAD cells to investigate changes in their biological process-

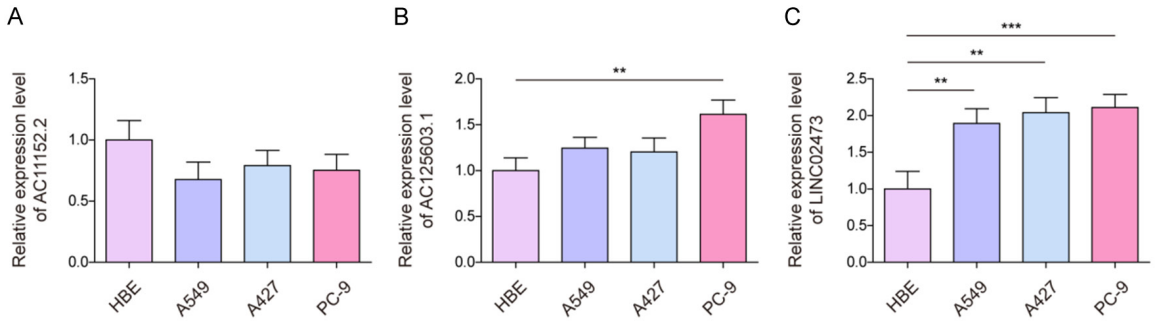


Figure 3. Expression levels of three lncRNAs in LUAD cell lines determined using qRT-PCR. A. Expression level of AC111152.2. B. Expression level of AC125603.1. C. Expression level of LINC02473. Note: **P < 0.01, ***P < 0.001.

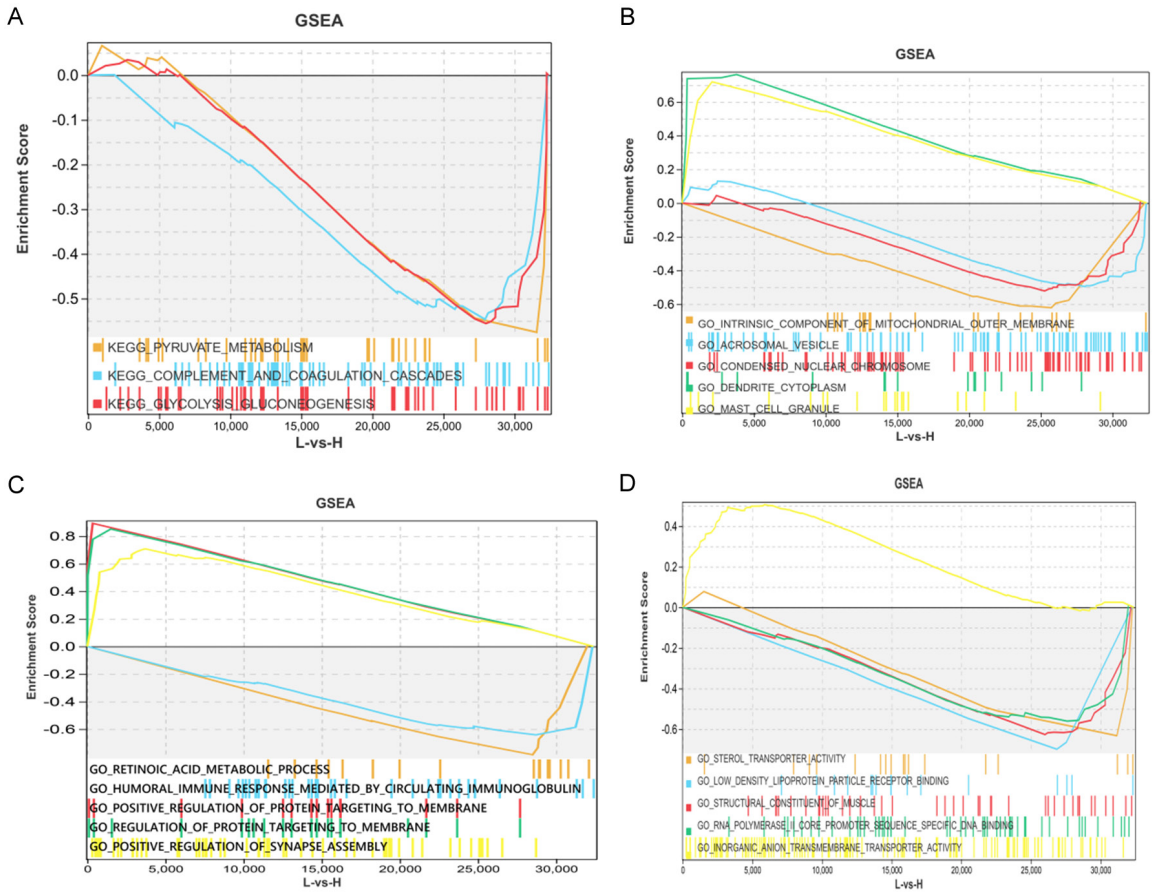


Figure 4. Analysis of potential functions of LINC02473 biology. A. KEGG database showing enrichment analysis of metabolic pathways and signaling pathways associated with LINC02473 expression changes. B. Enrichment of LINC02473 related cellular components (CC). C. Enrichment analysis of LINC02473-related biological processes (BP). D. Enrichment analysis of LINC02473-related molecular function (MF).

es. The results obtained by performing CCK-8, colony formation, and EdU assays showed that there was a significant inhibition of cell viability, colony formation ability, and proliferation with the transfection of si-LINC02473 (**Figure 6A-C**). Conversely, flow cytometry analysis demonstrated a significant increase in the apoptosis rate of si-LINC02473-transfected cells (**Figure 6D**). Moreover, by examining the glucose uptake and lactate production in transfected cells (**Figure 6E**, **6F**), we observed a noteworthy reduction in both parameters in si-LINC02473-

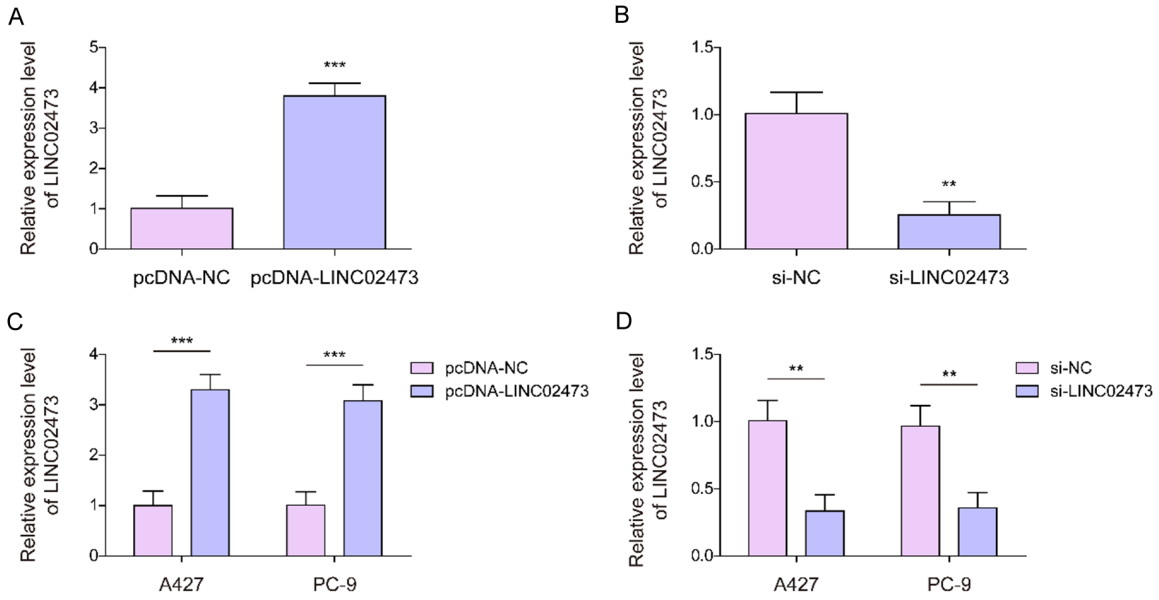


Figure 5. Construction and validation of LINC02473 overexpression and knockdown constructs. A, B. Construction of LINC02473 overexpression and knockdown constructs. C, D. Validation of LINC02473 expression following transfection into A427 and PC-9 cells. Note: $^{**}P < 0.01$, $^{***}P < 0.001$.

transfected cells. In addition, ECAR analysis showed that LINC02473 knockdown decreased ECAR (Figure S2A). Remarkably, independent transfection with pcDNA-LINC02473 produced opposite effects on these biological processes. This indicates the involvement of LINC02473 in the growth and glycolysis processes of LUAD cells.

FTO-mediated demethylation of m6A regulates LINC02473 expression

RNA metabolism and function in cancer are heavily influenced by post-transcriptional m6A modification. We hypothesized that m6A modification may contribute to the upregulation of LINC02473 in LUAD. With high confidence, the SRAMP database predicted two m6A modification sites within the LINC02473 transcript sequence (**Figure 7A**). Furthermore, MeRIP-qPCR assays revealed that LINC02473 had lower m6A enrichment in LUAD cells (A549, A427, and PC-9) than in HBE cells (**Figure 7B**). WB confirmed the high expression of FTO in LUAD cells (**Figure 7C**). Then we overexpressed and knocked down FTO and examined the efficiency of overexpression and knockdown (**Figure 7D**). meRIP-qPCR showed that FTO overexpression decreased the m6A modification of LINC02473, whereas downregulation of FTO resulted in an increase in the m6A modification of LINC02473 (**Figure 7E**, **7F**). Meanwhile, FTO overexpression significantly elevated LINC02473 expression, while FTO knockdown reduced its expression (**Figure 7G**). The above results suggest that FTO acts as an upstream regulator of LINC02473.

To further determine the specific m6A sites mediating FTO regulation and the effect on LINC02473 stability, we constructed single- and double-site mutants of the m6A sites in LINC02473 (Figure S3A). Dual-luciferase reporter assays showed that FTO overexpression significantly increased the luciferase activity of LINC02473-WT, whereas FTO knockdown had the opposite effect. Mutation of either single m6A site partially reduced the FTO-induced increase in luciferase activity, whereas double mutation abolished the effect of FTO (Figure S3B, S3C). These results indicate that FTO regulation of LINC02473 depends on the two m6A sites at positions 290 and 2271. Actinomycin D assays showed that FTO overexpression increased LINC02473 stability, whereas FTO knockdown decreased it (Figure S3D). These observations strongly suggest that FTO regulates the stability of LINC02473 through m6A demethylation, thereby promoting its expression.

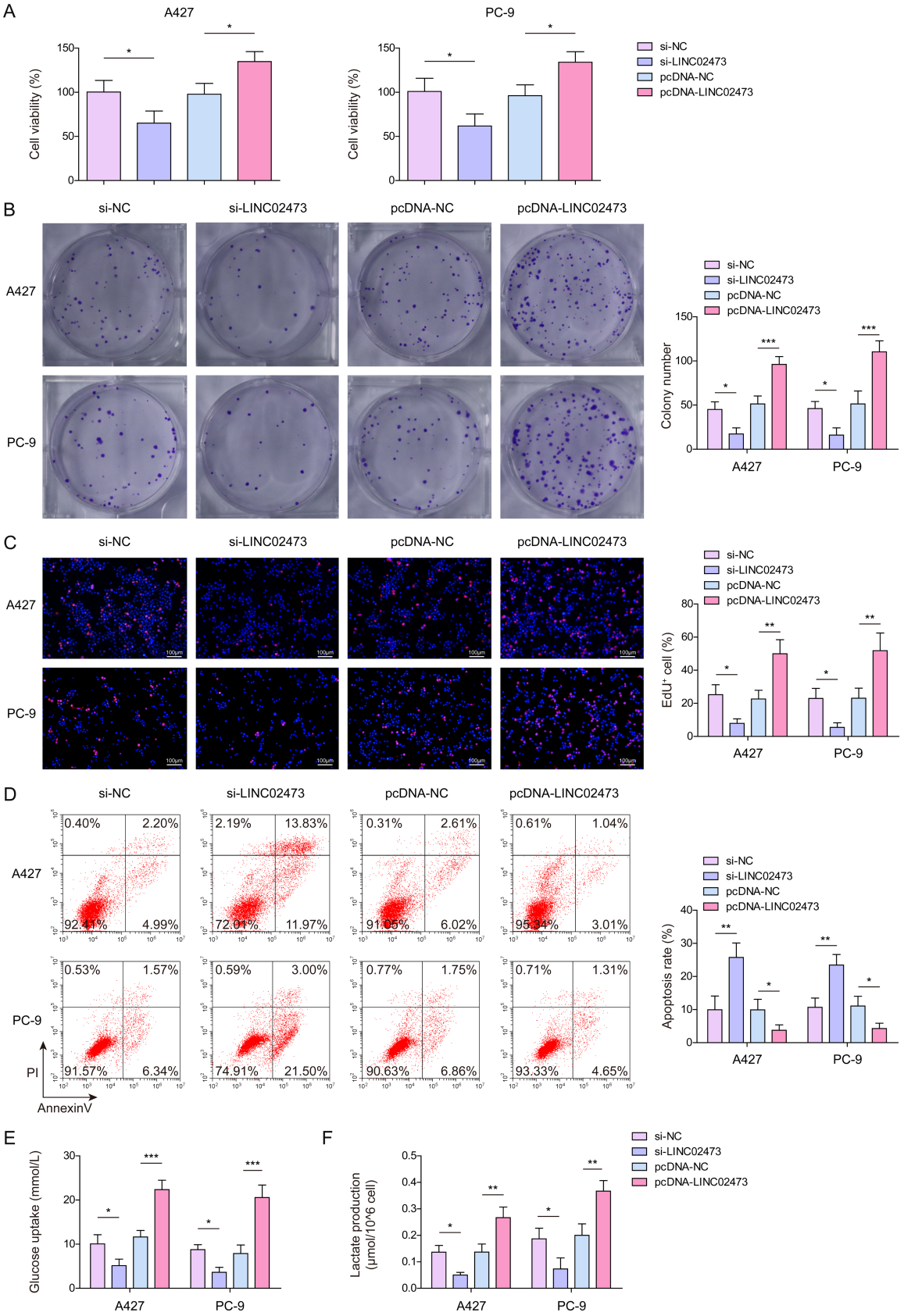


Figure 6. Effects of LINC02473 overexpression or knockdown on LUAD cell growth and glycolysis. A. Cell viability assessed using the CCK-8 assay. B. Colony-forming ability assessed using the colony formation assay. C. Cell prolifera-

tion assessed using the EdU incorporation assay (Scale bar, 100 μm). D. Cell apoptosis assessed by flow cytometry. E, F. Glucose and lactate levels. Note: *P < 0.05, **P < 0.01, ***P < 0.001.

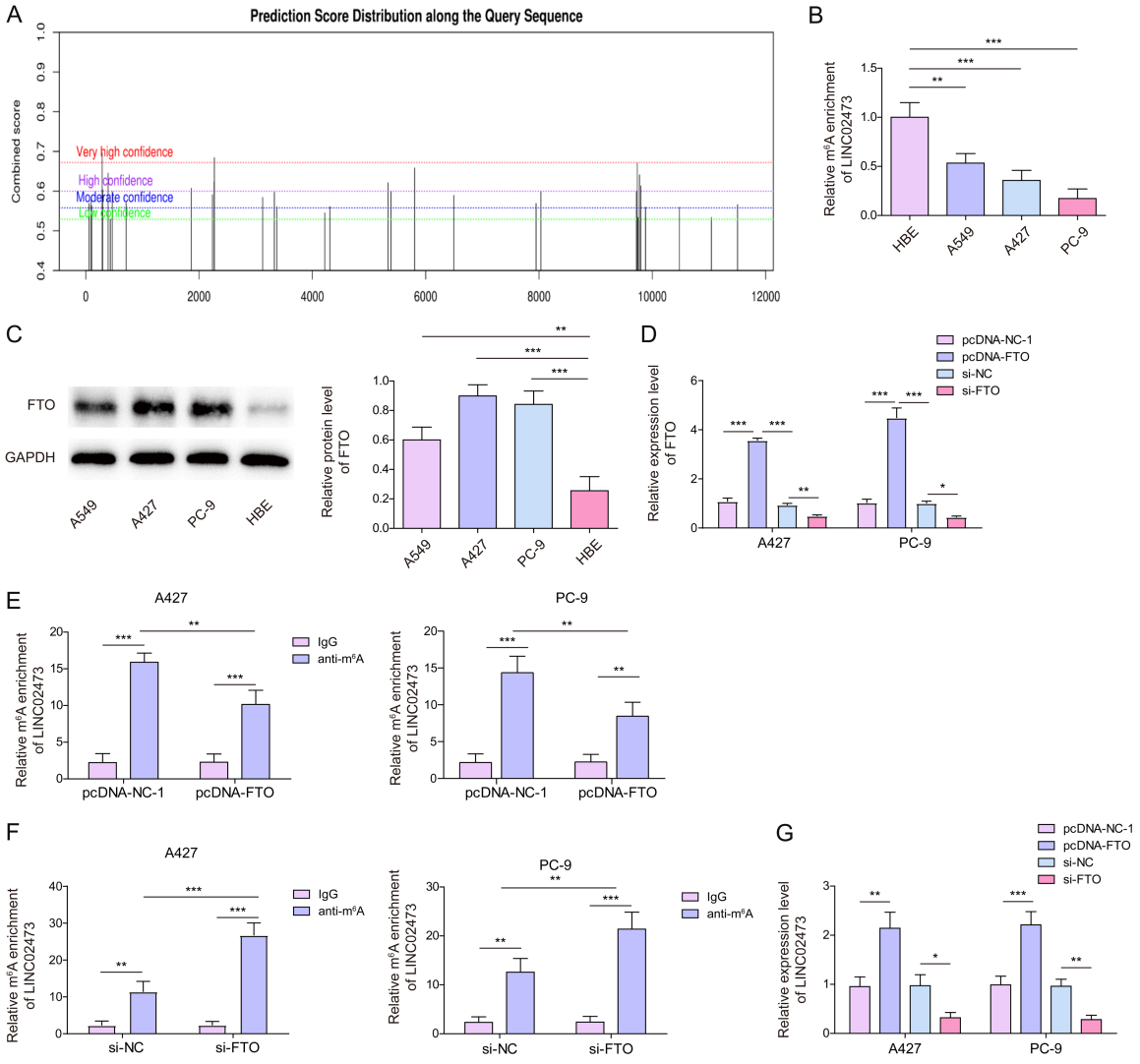


Figure 7. FTO-mediated m6A demethylation regulates LINC02473 expression. A. Prediction of potential m6A modification sites in LINC02473 using SRAMP. B. Assessment of LINC02473 m6A level in LUAD cells (A549, A427, and PC-9) and HBE cells. C. Western blot analysis of FTO protein expression in LUAD cells (A549, A427, and PC-9) and HBE cells. D. Validation of FTO overexpression and knockdown by qRT-PCR. E, F. Assessment of LINC02473 m6A enrichment following FTO overexpression or knockdown in A427 and PC-9 cells. G. Effects of FTO overexpression or knockdown on LINC02473 expression. Note: *P < 0.05, **P < 0.01, ***P < 0.001.

LINC02473 targets miR-340-5p and negatively regulates expression in LUAD cells

To investigate the downstream molecular mechanism of LINC02473 in LUAD, we first considered the ceRNA hypothesis, which proposes that lncRNAs act as miRNA sponges by binding miRNAs and recruiting them to the RNA-induced silencing complex (RISC) [18]. We therefore performed an Ago2-RIP assay in A427 and PC-9 cells. The results showed that both LINC02473 and miR-340-5p were enriched in Ago2-containing ribonucleoprotein complexes (**Figure 8A**, **8B**), supporting the possibility that LINC02473 may function as a ceRNA to sponge miR-340-5p.

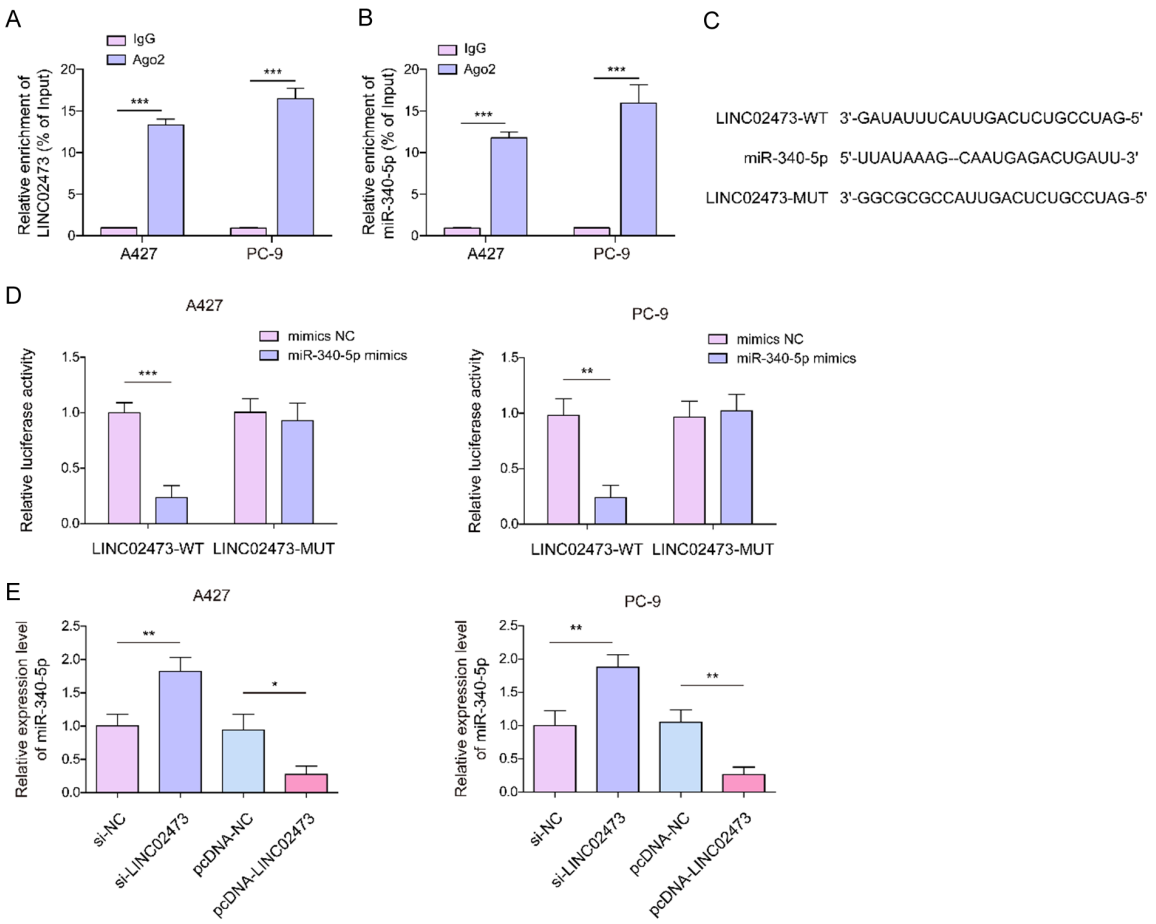


Figure 8. LINC02473 directly interacts with miR-340-5p and negatively regulates its expression. A, B. RNA immunoprecipitation (RIP) assays using an anti-Ago2 antibody in A427 and PC-9 cells, showing enrichment of LINC02473 and miR-340-5p in Ago2-containing complexes. C. Predicted binding site between miR-340-5p and LINC02473 obtained using an online prediction tool. D. Dual-luciferase reporter assay showing the effect of miR-340-5p mimics on the luciferase activity of the LINC02473-WT reporter. E. qRT-PCR analysis of miR-340-5p expression following LINC02473 overexpression or knockdown in LUAD cells. Note: $^{*}P < 0.05$, $^{**}P < 0.01$, $^{***}P < 0.001$.

To further identify the potential miRNA targets of LINC02473, we performed miRNA prediction using miRDB. The bioinformatics analysis indicated that miR-340-5p was a potential target of LINC02473 (**Figure 8C**). We then validated this predicted interaction using a dual-luciferase reporter assay. Transfection with miR-340-5p mimics significantly altered the luciferase activity of the LINC02473-WT reporter in A427 and PC-9 cells (**Figure 8D**). Furthermore, suppression of LINC02473 resulted in increased miR-340-5p expression, whereas ectopic expression of LINC02473 significantly reduced miR-340-5p levels (**Figure 8E**). Collectively, these observations suggest that LINC02473 may act as a competing endogenous RNA by binding to miR-340-5p and negatively regulating its abundance in LUAD cells.

FTO promotes LUAD cell growth and glycolysis through the LINC02473/miR-340-5p axis

To verify the regulatory relationship of the FTO/LINC02473/miR-340-5p axis, we performed rescue experiments. In A427 and PC-9 cells, knockdown of FTO alone or transfection with miR-340-5p mimics alone significantly inhibited colony formation (**Figure 9A**) and proliferation (**Figure 9B**), promoted apoptosis (**Figure 9C**), and reduced glucose uptake and lactate production (**Figure 9D**, **9E**). Further overexpression of LINC02473 on the basis of FTO knockdown or miR-340-5p overexpression signifi-

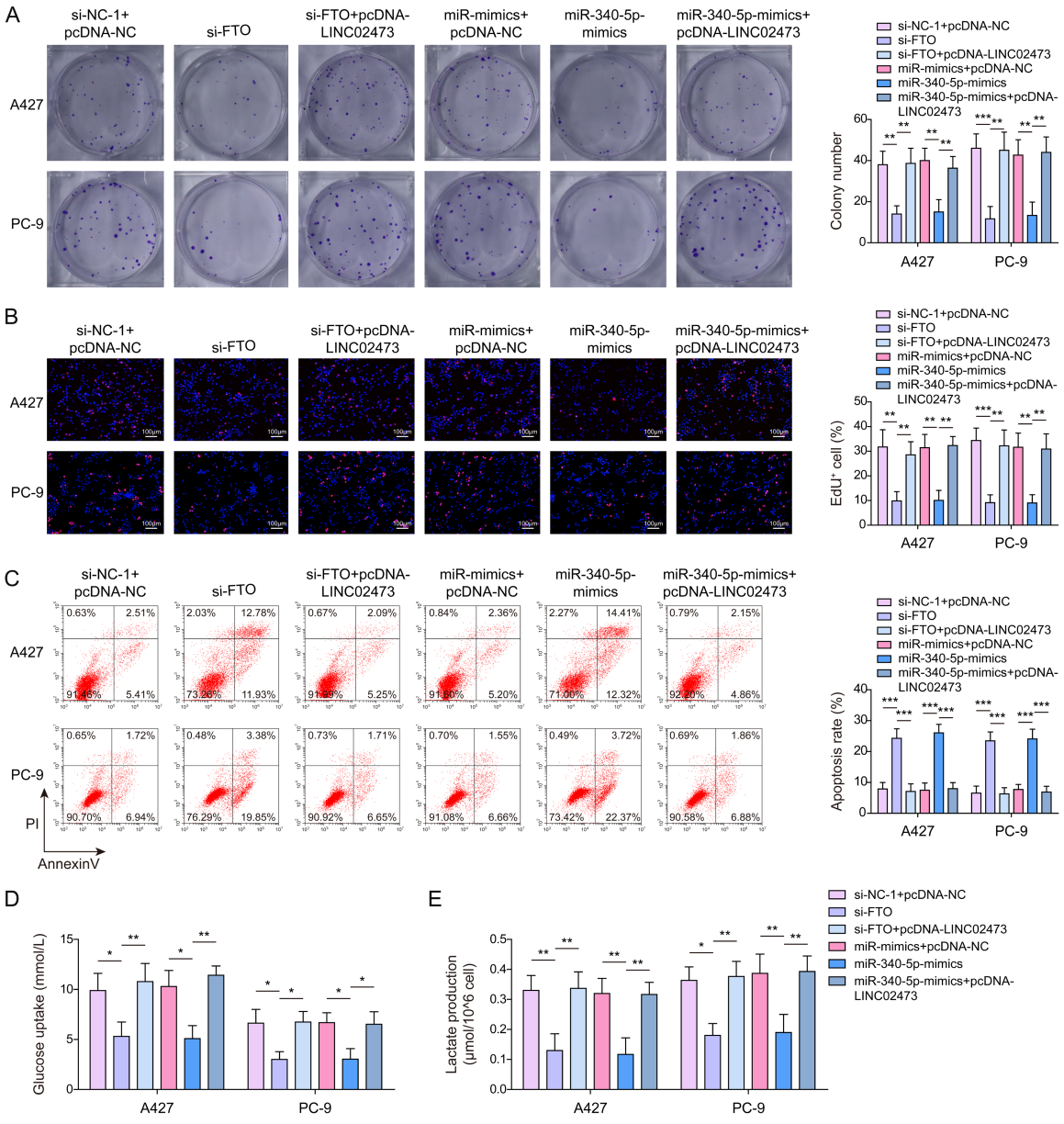


Figure 9. FTO promotes LUAD cell growth and glycolysis through the LINC02473/miR-340-5p axis. A. The colony formation assay was performed to evaluate the impact of co-transfection on the ability of LUAD cells to form colonies. B. The EdU incorporation assay was conducted to examine the effect of co-transfection on the proliferative capacity of LUAD cells (Scale bar, 100 μm). C. Flow cytometry analysis was employed to assess the effect of co-transfection on the rate of apoptosis in LUAD cells. D. The glucose content in LUAD cells was measured after co-transfection. E. The lactate content in LUAD cells was determined following co-transfection. Note: $^{*}P < 0.05$, $^{**}P < 0.01$, $^{***}P < 0.001$.

cantly restored the malignant phenotype and glycolytic level of the cells (**Figure 9A-E**). In addition, ECAR analysis showed that knockdown of FTO alone or transfection with miR-340-5p mimics alone decreased ECAR, whereas further overexpression of LINC02473 enhanced ECAR (Figure S2B). These results collectively indicate that FTO promotes the growth and glycolysis of LUAD cells by regulating the LINC02473/miR-340-5p axis.

Discussion

Over recent decades, molecular oncology research has largely focused on elucidating the functions of protein-coding genes [19]. With the

rapid development of high-throughput sequencing, however, increasing attention has been directed toward lncRNAs, which were once considered transcriptional or genomic "noise". Subsequent studies have demonstrated that lncRNAs are widely transcribed in mammalian cells and participate in the regulation of numerous biological processes and human diseases [20]. These findings have substantially expanded current understanding of the functional complexity of the non-coding genome. LncRNAs are widely expressed in mammalian cells and have been linked to human diseases [21]. As a result, these lncRNAs are considered valuable biomarkers and potential therapeutic targets due to their tissue specificity and essential functions in reshaping tumor cell proliferation and survival [22, 23].

In this study, we analyzed publicly available sequencing datasets to examine the expression of lncRNAs in LUAD tumor samples and neighboring normal samples. We identified a significant number of lncRNAs that were expressed differently in the tumor samples compared to the normal samples. Finding subsets of lncRNAs that are associated with LUAD has been a difficult task, as there are numerous lncRNAs to consider. While the functions of certain lncRNAs, such as LINC01614 and LINC01977, have been studied and shown to be involved in the malignant behavior of LUAD, the majority of lncRNAs in LUAD biology have not been fully characterized. Through examination of the array-based datasets GSE138172 and GSE196584, we have discovered a novel lncRNA called LINC02473, which exhibits significant upregulation in LUAD tumors. Although the role of lncRNAs in LUAD has been reported previously [24, 25], there is an absence of substantial research on this topic. Consequently, the exact biological function of LINC02473 in LUAD development, as well as the underlying mechanisms responsible for its dysregulation, are still unknown. To obtain further insight into the biological role of LINC02473 in LUAD, samples were categorized into high- and low-LINC02473-expression groups, followed by gene set enrichment analysis (GSEA). Functional enrichment analysis indicated that variation in LINC02473 expression was closely associated with pathways involved in cellular activity and glycolytic metabolism. These observations, together with the elevated expression of LINC02473 in LUAD, suggest that this lncRNA may contribute to tumor progression by modulating the biological behavior and metabolic characteristics of LUAD cells.

The mechanism by which LINC02473 affects LUAD is further explored through an extensive study. Downregulation of LINC02473 was found to significantly reduce the viability and proliferation of LUAD cells as well as the colony formation capability. Moreover, apoptosis was induced. On the other hand, glucose and lactate levels were significantly reduced as a consequence of LINC02473 down-regulation. However, pcDNA-LINC02473 transfection reversed the above-mentioned cellular activities. In addition, ECAR analysis showed that LINC02473 knockdown decreased ECAR, whereas LINC02473 overexpression increased ECAR, further supporting the involvement of LINC02473 in glycolytic regulation. In summary, all current results have shown that LINC02473 is critically involved in the development of LUAD by increasing cell proliferation and affecting glucose metabolism. Therefore, LINC02473 is a promising candidate therapeutic target for LUAD. It is important to note that previous research by Hong et al. [26] showed that SP1 transcription factor stimulated by ribosome binding increased the expression level of lncRNA ENO1-IT1 by increasing SP1 binding to its promoter region. This process led to glycolysis upregulation and biological changes in colon cancer cells. Moreover, Wang et al. [27] showed that LINRIS was an independent biomarker of colorectal cancer (CRC). Also, by modulating the LINRIS-IGF2BP2-MYC axis, glycolysis could be regulated in CRC cells. Therefore, it is clear that all the above-mentioned studies demonstrate the major effect of lncRNAs on the development of diseases via the regulation of the glycolytic pathway in tumor cells.

Compared with other epigenetic regulatory mechanisms, investigation of m6A modification provides an additional molecular perspective for understanding the post-transcriptional regulation of RNA [28]. Research has shown that m6A modification of messenger RNAs (mRNAs) is crucial for cellular growth, metabolism, and differentiation [29]. By regulating abnormal m6A modifications of specific mRNAs, cancer cells sustain their ability to regenerate and proliferate. Recent investigations have centered

on the role of m6A methylation in regulating mRNAs in cancer cells, and some lncRNAs modified by m6A, such as lncRNA SNHG17 [30], lncRNA ZNRD1-AS1 [31], and lncRNA MALAT1 [32], have been implicated. However, the mechanisms through which m6A modifications control lncRNAs in LUAD are not well understood. By applying bioinformatics analysis and conducting the MeRIP assay, our investigation revealed the existence of m6A-modified transcripts derived from the LINC02473 gene in LUAD cells. In comparison to the normal HBE cell line, LUAD cells displayed a decreased m6A modification level of LINC02473, an effect that was regulated by the m6A demethylase FTO. To further define the specific m6A sites mediating FTO regulation, we constructed single- and double-site mutants of the m6A sites in LINC02473. Dual-luciferase reporter assays showed that FTO regulation of LINC02473 depends on the two m6A sites at positions 290 and 2271, and actinomycin D assays confirmed that FTO overexpression increased LINC02473 stability, whereas FTO knockdown decreased it. To the best of our knowledge, this study represents the first report highlighting the ability of m6A to regulate lncRNA stability in LUAD cells, thus augmenting our comprehension of the pivotal role played by lncRNAs in the progression of LUAD.

FTO is an m6A demethylase which was originally found to be involved in tumor formation in acute myeloid leukemia (AML) [33]. Subsequent studies have indicated that aberrant activity of FTO promotes the onset and development of various tumors. The mechanism by which this occurs includes FTO demethylating specific mRNAs and lncRNAs via m6A-mediated RNA modifications using reader proteins [34, 35]. In the present study, LINC02473 was identified as a previously unrecognized downstream target of FTO. FTO protein expression was markedly higher in LUAD cell lines than in the corresponding controls. Moreover, the FTO-mediated demethylation of m6A is considered a crucial regulatory mechanism that affects LINC02473 stability. Consistent with these molecular findings, depletion of FTO restrained LUAD cell proliferation and growth, enhanced apoptosis, and attenuated glycolytic activity. Additionally, functional rescue experiments showed that overexpression of LINC02473 partially rescued the suppressed cell growth and reduced glycolytic capacity caused by FTO knockdown in LUAD cells. Taken together, these results support a tumor-promoting role for FTO in LUAD and suggest that its oncogenic effects may, at least in part, be mediated through regulation of LINC02473.

Studies have increasingly shown that lncRNAs exhibit the ability to function as “sponges” for miRNAs, thereby regulating the expression of miRNAs [36]. Accumulating evidence suggests that lncRNAs can modulate miRNA activity by functioning as molecular sponges [36]. In particular, cytoplasmic lncRNAs may act as competing endogenous RNAs (ceRNAs), competitively interacting with miRNAs and thereby altering the expression of genes targeted by these miRNAs [37]. The regulatory interplay between lncRNAs and miRNAs has been documented in numerous biological and pathological processes, including tumorigenesis [38, 39]. The interplay between ceRNAs relies on the complementary binding of miRNA response elements (MREs), which form the foundation of this intricate network of interactions [40]. In our investigation, we initially identified miR-340-5p as one of the miRNAs that interacts with LINC02473 through both bioinformatics analysis and experimental validation. MiR-340-5p has been reported to exert tumor-suppressive effects by limiting cancer cell proliferation and metastatic potential in multiple malignancies. The interactions between LINC02473 and miR-340-5p were studied through co-transfection assays in this study, revealing their involvement in regulating LUAD. Compared with si-FTO or miR-340-5p mimics alone, which inhibited proliferation and colony formation, promoted apoptosis, and reduced ECAR, further LINC02473 overexpression partially reversed these effects, confirming that FTO promotes glycolysis via the LINC02473/miR-340-5p axis.

Despite this, several limitations should be highlighted while investigating the molecular mechanism of LINC02473 in LUAD and its interaction with miR-340-5p. First, the current study is mostly based on bioinformatics analysis and in vitro experiments. No in vivo animal models or clinical trials were included. Second, although LINC02473 has been shown to play an important role in proliferation and glycolysis in LUAD by modulating miR-340-5p and FTO-mediated m6A demethylation, more research is needed

to identify the specific target genes and related signaling pathways. Therefore, further in vivo and clinical studies, together with additional mechanistic investigations, are needed to validate these findings and clarify the downstream targets and pathways, thereby substantiating the potential clinical application and diagnostic significance of LINC02473 in LUAD treatment.

Conclusion

Collectively, this study reveals that FTO-mediated m6A demethylation promotes LUAD proliferation and glycolysis and inhibits apoptosis through the LINC02473/miR-340-5p axis. Mechanistically, FTO-mediated m6A demethylation enhances LINC02473 expression, and LINC02473 binds miR-340-5p to inhibit miR-340-5p expression. This regulatory cascade links epigenetic m6A modification, lncRNA-mediated miRNA sponging, and metabolic reprogramming in LUAD. These findings deepen our understanding of LUAD pathogenesis and highlight the LINC02473/miR-340-5p axis as a potential therapeutic target. Targeting this axis may provide new opportunities for precision treatment of LUAD.

Acknowledgements

We thank all the researchers who participated in the experiment and data processing. This work was supported by Hainan Province Science and Technology Special Fund (No. ZDYF2023SHFZ133).

Disclosure of conflict of interest

None.

Address correspondence to: Yihui Fu, Department of Pulmonary and Critical Care Medicine, Hainan General Hospital (Hainan Affiliated Hospital of Hainan Medical University), No. 19, Xiuhua Road, Xiuying District, Haikou 570311, Hainan, P. R. China. Tel: +86-0898-68642548; Fax: +86-0898-6864-2548; E-mail: hysfy4449@muhn.edu.cn

References

[1] Karasaki T, Moore DA, Veeriah S, Naceur-Lombardelli C, Toncheva A, Magno N, Ward S, Bakir MA, Watkins TBK, Grigoriadis K, Huebner A, Hill MS, Frankell AM, Abbosh C, Puttick C, Zhai H, Gimeno-Valiente F, Saghafinia S, Kanu N, Dietzen M, Pich O, Lim EL, Martínez-Ruiz C, Black JRM, Biswas D, Campbell BB, Lee C, Colliver E, Enfield KSS, Hessey S, Hiley CT, Zaccaria S, Litchfield K, Birkbak NJ, Cadieux EL, Demeulemeester J, Van Loo P, Adusumilli PS, Tan KS, Cheema W, Sanchez-Vega F, Jones DR, Rekhtman N, Travis WD, Hackshaw A, Marafioti T, Salgado R, Le Quesne J, Nicholson AG, McGranahan N, Swanton C and Jamal-Hanjani M; TRACERx Consortium. Evolutionary characterization of lung adenocarcinoma morphology in TRACERx. Nat Med 2023; 29: 833-845.

[2] Hill W, Lim EL, Weeden CE, Lee C, Augustine M, Chen K, Kuan FC, Marongiu F, Evans EJ Jr, Moore DA, Rodrigues FS, Pich O, Bakker B, Cha H, Myers R, van Maldegem F, Boumelha J, Veeriah S, Rowan A, Naceur-Lombardelli C, Karasaki T, Sivakumar M, De S, Caswell DR, Nagano A, Black JRM, Martínez-Ruiz C, Ryu MH, Huff RD, Li S, Favé MJ, Magness A, Suárez-Bonnet A, Priestnall SL, Lüchtenborg M, Lavelle K, Pethick J, Hardy S, McRonald FE, Lin MH, Troccoli CI, Ghosh M, Miller YE, Merrick DT, Keith RL, Al Bakir M, Bailey C, Hill MS, Saal LH, Chen Y, George AM, Abbosh C, Kanu N, Lee SH, McGranahan N, Berg CD, Sasieni P, Houlston R, Turnbull C, Lam S, Awadalla P, Grönroos E, Downward J, Jacks T, Carlsten C, Malanchi I, Hackshaw A, Litchfield K; TRACERx Consortium, DeGregori J, Jamal-Hanjani M and Swanton C. Lung adenocarcinoma promotion by air pollutants. Nature 2023; 616: 159-167.

[3] Rivera-Ortega P and Molina-Molina M. Interstitial lung diseases in developing countries. Ann Glob Health 2019; 85: 4.

[4] Zlotorynski E. Non-Coding RNA: a class of their own. Nat Rev Mol Cell Biol 2017; 18: 71.

[5] Nair L, Chung H and Basu U. Regulation of long non-coding RNAs and genome dynamics by the RNA surveillance machinery. Nat Rev Mol Cell Biol 2020; 21: 123-136.

[6] Lorenzi L, Chiu HS, Avila Cobos F, Gross S, Volders PJ, Cannoodt R, Nuytens J, Vanderheyden K, Anckaert J, Lefever S, Tay AP, de Bony EJ, Trypsteen W, Gysens F, Vromman M, Goovaerts T, Hansen TB, Kuersten S, Nijs N, Taghon T, Vermaelen K, Bracke KR, Saeys Y, De Meyer T, Deshpande NP, Anande G, Chen TW, Wilkins MR, Unnikrishnan A, De Preter K, Kjems J, Koster J, Schroth GP, Vandesompele J, Sumazin P and Mestdagh P. The RNA Atlas expands the catalog of human non-coding RNAs. Nat Biotechnol 2021; 39: 1453-1465.

[7] Anastasiadou E, Jacob LS and Slack FJ. Non-coding RNA networks in cancer. Nat Rev Cancer 2018; 18: 5-18.

[8] Zhang Y, Dong X, Guo X, Li C, Fan Y, Liu P, Yuan D, Ma X, Wang J, Zheng J, Li H and Gao P. LncRNA-BC069792 suppresses tumor progres-

sion by targeting KCNQ4 in breast cancer. Mol Cancer 2023; 22: 41.
[9] He Y, Jiang X, Duan L, Xiong Q, Yuan Y, Liu P, Jiang L, Shen Q, Zhao S, Yang C and Chen Y. LncRNA PKMYT1AR promotes cancer stem cell maintenance in non-small cell lung cancer via activating Wnt signaling pathway. Mol Cancer 2021; 20: 156.
[10] Xue C, Chu Q, Zheng Q, Jiang S, Bao Z, Su Y, Lu J and Li L. Role of main RNA modifications in cancer: N6-methyladenosine, 5-methylcytosine, and pseudouridine. Signal Transduct Target Ther 2022; 7: 142.
[11] Liu J, Yue Y and He C. Preparation of human nuclear RNA m6A methyltransferases and demethylases and biochemical characterization of their catalytic activity. Methods Enzymol 2015; 560: 117-130.
[12] Xiao S, Guo S, Han J, Sun Y, Wang M, Chen Y, Fang X, Yang F, Mu Y, Zhang L, Ding Y, Zhang N, Jiang H, Chen K, Zhao K, Luo C and Chen S. High-Throughput-Methyl-Reading (HTMR) assay: a solution based on nucleotide methyl-binding proteins enables large-scale screening for DNA/RNA methyltransferases and demethylases. Nucleic Acids Res 2022; 50: e9.
[13] Covelo-Molares H, Obrdlik A, Poštulková I, Dohnálková M, Gregorová P, Ganji R, Potěšil D, Gawriyski L, Varjosalo M and Vaňáčová Š. The comprehensive interactomes of human adenosine RNA methyltransferases and demethylases reveal distinct functional and regulatory features. Nucleic Acids Res 2021; 49: 10895-10910.
[14] Shang L, Zhang W, Wu H, Wu R and Chen R. Diagnostic value of FTO combined with CEA or CYFRA21-1 in nonsmall cell lung cancer. Evid Based Complement Alternat Med 2021; 2021: 1436088.
[15] Gao L, Wang A, Chen Y, Cai X, Li Y, Zhao J, Zhang Y, Zhang W, Zhu J, Zeng Y, Liu Z and Huang JA. FTO facilitates cancer metastasis by modifying the m6A level of FAP to induce integrin/FAK signaling in non-small cell lung cancer. Cell Commun Signal 2023; 21: 311.
[16] Wang Y, He R and Ma L. Characterization of lncRNA-associated ceRNA network to reveal potential prognostic biomarkers in lung adenocarcinoma. Front Bioeng Biotechnol 2020; 8: 266.
[17] Liu S, Wang Z, Zhu R, Wang F, Cheng Y and Liu Y. Three differential expression analysis methods for RNA sequencing: limma, EdgeR, DESeq2. J Vis Exp 2021.
[18] Nejadi Orang F and Abdoli Shadbad M. Competing endogenous RNA networks and ferroptosis in cancer: novel therapeutic targets. Cell Death Dis 2024; 15: 357.
[19] Tsimberidou AM, Kahle M, Vo HH, Baysal MA, Johnson A and Meric-Bernstam F. Molecular tumour boards - current and future considerations for precision oncology. Nat Rev Clin Oncol 2023; 20: 843-863.
[20] Oxnard GR, West HJ and King JC. Improving molecular oncology by making results available to patients. JAMA Oncol 2019; 5: 1689-1690.
[21] Rion N and Rüegg MA. LncRNA-encoded peptides: more than translational noise? Cell Res 2017; 27: 604-605.
[22] Li Z, Zhao X, Zhou Y, Liu Y, Zhou Q, Ye H, Wang Y, Zeng J, Song Y, Gao W, Zheng S, Zhuang B, Chen H, Li W, Li H, Li H, Fu Z and Chen R. The long non-coding RNA HOTTIP promotes progression and gemcitabine resistance by regulating HOXA13 in pancreatic cancer. J Transl Med 2015; 13: 84.
[23] Yang M, Lu H, Liu J, Wu S, Kim P and Zhou X. lncRNAfunc: a knowledgebase of lncRNA function in human cancer. Nucleic Acids Res 2022; 50: D1295-D1306.
[24] Liu T, Han C, Fang P, Ma Z, Wang X, Chen H, Wang S, Meng F, Wang C, Zhang E, Dong G, Zhu H, Yin W, Wang J, Zuo X, Qiu M, Wang J, Qian X, Shen H, Xu L, Hu Z and Yin R. Cancer-associated fibroblast-specific lncRNA LINC01614 enhances glutamine uptake in lung adenocarcinoma. J Hematol Oncol 2022; 15: 141.
[25] Zhang T, Xia W, Song X, Mao Q, Huang X, Chen B, Liang Y, Wang H, Chen Y, Yu X, Zhang Z, Yang W, Xu L, Dong G and Jiang F. Super-enhancer hijacking LINC01977 promotes malignancy of early-stage lung adenocarcinoma addicted to the canonical TGF-β/SMAD3 pathway. J Hematol Oncol 2022; 15: 114.
[26] Hong J, Guo F, Lu SY, Shen C, Ma D, Zhang X, Xie Y, Yan T, Yu T, Sun T, Qian Y, Zhong M, Chen J, Peng Y, Wang C, Zhou X, Liu J, Liu Q, Ma X, Chen YX, Chen H and Fang JY. F. nucleatum targets lncRNA ENO1-IT1 to promote glycolysis and oncogenesis in colorectal cancer. Gut 2021; 70: 2123-2137.
[27] Wang Y, Lu JH, Wu QN, Jin Y, Wang DS, Chen YX, Liu J, Luo XJ, Meng Q, Pu HY, Wang YN, Hu PS, Liu ZX, Zeng ZL, Zhao Q, Deng R, Zhu XF, Ju HQ and Xu RH. LncRNA LINRIS stabilizes IGF2BP2 and promotes the aerobic glycolysis in colorectal cancer. Mol Cancer 2019; 18: 174.
[28] Wang Y, Li M, Zhang L, Chen Y and Zhang S. m6A demethylase FTO induces NELL2 expression by inhibiting E2F1 m6A modification leading to metastasis of non-small cell lung cancer. Mol Ther Oncolytics 2021; 21: 367-376.
[29] Diao MN, Zhang XJ and Zhang YF. The critical roles of m6A RNA methylation in lung cancer:

from mechanism to prognosis and therapy. Br J Cancer 2023; 129: 8-23.
[30] Zhang H, Wang SQ, Wang L, Lin H, Zhu JB, Chen R, Li LF, Cheng YD, Duan CJ and Zhang CF. m6A methyltransferase METTL3-induced lncRNA SNHG17 promotes lung adenocarcinoma gefitinib resistance by epigenetically repressing LATS2 expression. Cell Death Dis 2022; 13: 657.
[31] Wang J, Tan L, Yu X, Cao X, Jia B, Chen R and Li J. lncRNA ZNRD1-AS1 promotes malignant lung cell proliferation, migration, and angiogenesis via the miR-942/TNS1 axis and is positively regulated by the m(6)A reader YTHDC2. Mol Cancer 2022; 21: 229.
[32] Li C, Liu J, Lyu Y, Ling S and Luo Y. METTL16 inhibits the malignant progression of epithelial ovarian cancer through the lncRNA MALAT1/β-catenin axis. Anal Cell Pathol (Amst) 2023; 2023: 9952234.
[33] Huang Y, Su R, Sheng Y, Dong L, Dong Z, Xu H, Ni T, Zhang ZS, Zhang T, Li C, Han L, Zhu Z, Lian F, Wei J, Deng Q, Wang Y, Wunderlich M, Gao Z, Pan G, Zhong D, Zhou H, Zhang N, Gan J, Jiang H, Mulloy JC, Qian Z, Chen J and Yang CG. Small-molecule targeting of oncogenic FTO demethylase in acute myeloid leukemia. Cancer Cell 2019; 35: 677-691, e10.
[34] Tao L, Mu X, Chen H, Jin D, Zhang R, Zhao Y, Fan J, Cao M and Zhou Z. FTO modifies the m6A level of MALAT and promotes bladder cancer progression. Clin Transl Med 2021; 11: e310.
[35] Zhou G, Yan K, Liu J, Gao L, Jiang X and Fan Y. FTO promotes tumour proliferation in bladder cancer via the FTO/miR-576/CDK6 axis in an m6A-dependent manner. Cell Death Discov 2021; 7: 329.
[36] Xu J, Feng L, Han Z, Li Y, Wu A, Shao T, Ding N, Li L, Deng W, Di X, Wang J, Zhang L, Li X, Zhang K and Cheng S. Extensive ceRNA-ceRNA interaction networks mediated by miRNAs regulate development in multiple rhesus tissues. Nucleic Acids Res 2016; 44: 9438-9451.
[37] Wu S, Zhong B, Yang Y, Wang Y and Pan Z. ceRNA networks in gynecological cancers progression and resistance. J Drug Target 2023; 31: 920-930.
[38] Zhang G, Li S, Lu J, Ge Y, Wang Q, Ma G, Zhao Q, Wu D, Gong W, Du M, Chu H, Wang M, Zhang A and Zhang Z. LncRNA MT1JP functions as a ceRNA in regulating FBXW7 through competitively binding to miR-92a-3p in gastric cancer. Mol Cancer 2018; 17: 87.
[39] Tang H, Xiong Q, Yin M, Feng H, Yao F, Xiao X, Hu F and Liao Y. LncRNA PVT1 delays skin photoaging by sequestering miR-551b-3p to release AQP3 expression via ceRNA mechanism. Apoptosis 2023; 28: 912-924.
[40] Guo K, Qian K, Shi Y, Sun T and Wang Z. LncRNA-MIAT promotes thyroid cancer progression and function as ceRNA to target EZH2 by sponging miR-150-5p. Cell Death Dis 2021; 12: 1097.

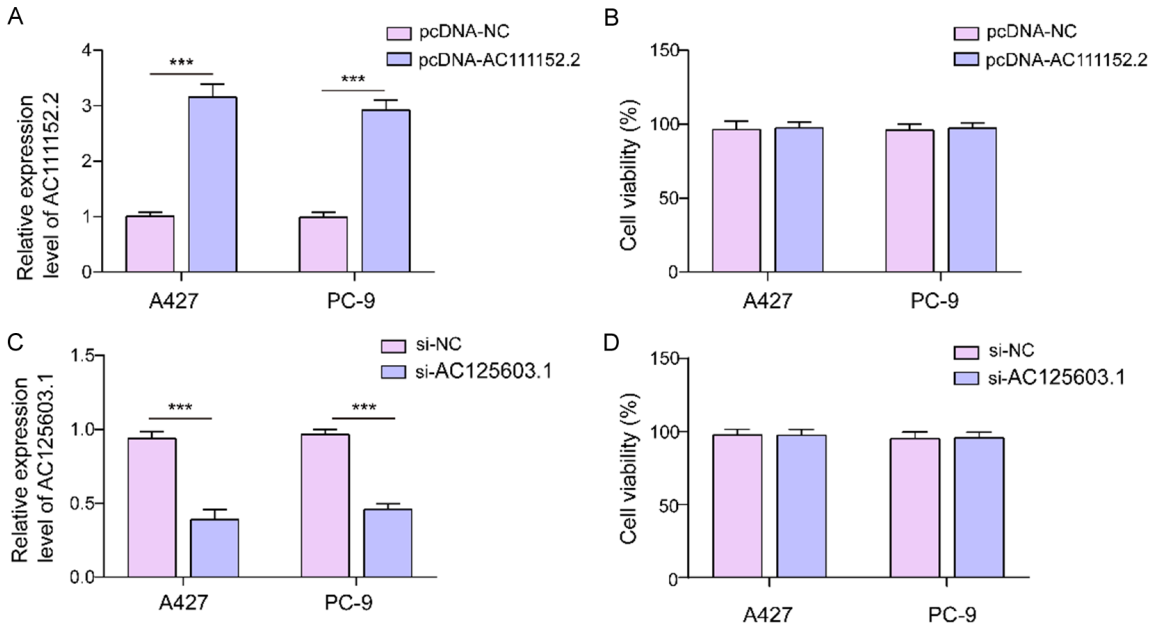


Figure S1. Effects of AC111152.2 and AC125603.1 on LUAD cell viability. A. The overexpression efficiency of pcDNA-AC111152.2 in A427 and PC-9 cells was analyzed by RT-qPCR. B. The effect of AC111152.2 overexpression on cell viability was evaluated by CCK-8. C. The knockdown efficiency of si-AC125603.1 in A427 and PC-9 cells was examined by RT-qPCR. D. The effect of AC125603.1 knockdown on cell viability was assessed by CCK-8. Note: ***P < 0.001.

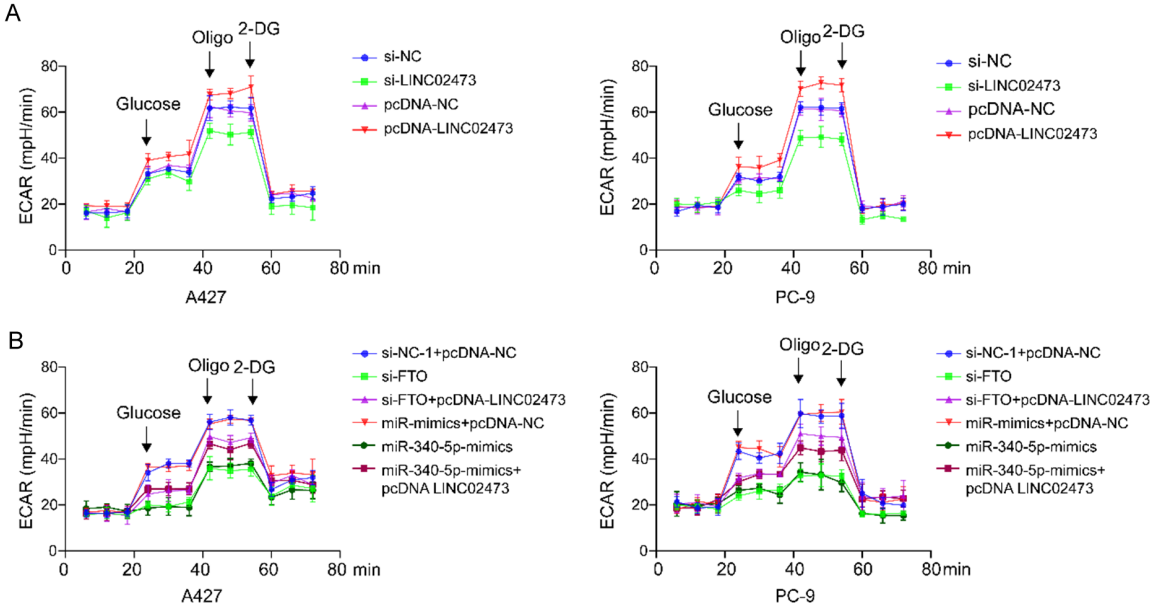


Figure S2. Effects of FTO, LINC02473 and miR-340-5p intervention on the extracellular acidification rate (ECAR) in LUAD cells. A. ECAR measurements in A427 and PC-9 cells transfected with si-NC, si-LINC02473, pcDNA-NC, or pcDNA-LINC02473. B. ECAR measurements in A427 and PC-9 cells transfected with si-NC-1 + pcDNA-NC, si-FTO, si-FTO + pcDNA-LINC02473, miR-mimics + pcDNA-NC, miR-340-5p mimics, or miR-340-5p mimics + pcDNA-LINC02473.

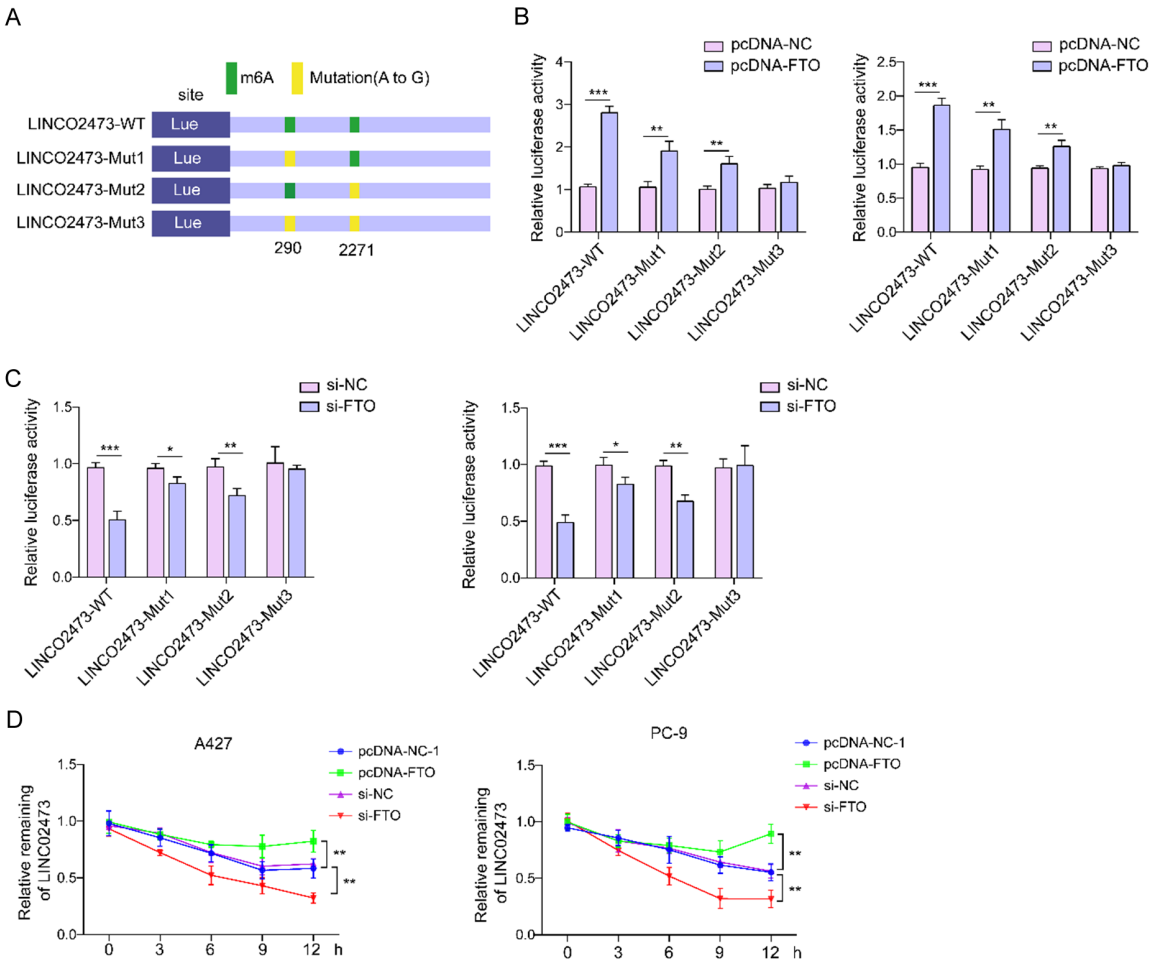


Figure S3. Identification of FTO-regulated m^{6}A sites in LINC02473 and the effects of FTO on LINC02473 stability. A. Schematic illustration of LINC02473 constructs carrying single- and double-site mutations at predicted m6A sites. B, C Dual-luciferase reporter assays in A427 and PC-9 cells transfected with pcDNA-NC-1, pcDNA-FTO, si-NC, or si-FTO to measure the luciferase activity of LINC02473-WT and m6A-site mutant reporters. D. Actinomycin D assay assessing LINC02473 stability in LUAD cells transfected with pcDNA-FTO or si-FTO. Note: $^*P < 0.05$, $^{**}P < 0.01$, $^{***}P < 0.001$.